

INVITED REVIEW

Positron emission tomography of the vulnerable atherosclerotic plaque in man – a contemporary review

Sune F. Pedersen^{1,2}, Anne Mette F. Hag^{1,2}, Thomas L. Klausen², Rasmus S. Ripa^{1,2}, Rasmus P. Bodholdt^{1,2} and Andreas Kjær^{1,2}

¹Cluster for Molecular Imaging, University of Copenhagen, and ²Department of Clinical Physiology, Nuclear Medicine & PET, Rigshospitalet, University of Copenhagen, Copenhagen, Denmark

Summary

Correspondence

Sune Folke Pedersen, MSc, Cluster for Molecular Imaging, University of Copenhagen, Blegdamsvej 3, 2200 Copenhagen N, Denmark
E-mail: sfolkep@sund.ku.dk

Accepted for publication

Received 27 June 2013;
accepted 21 October 2013

Key words

atherosclerosis; *in vivo*; molecular imaging; positron emission tomography; vulnerable plaque

Atherosclerosis is the primary underlying cause of cardiovascular disease (CVD). It is the leading cause of morbidity and mortality in the Western world today and is set to become the prevailing disease and major cause of death worldwide by 2020. In the 1950s surgical intervention was introduced to treat symptomatic patients with high-grade carotid artery stenosis due to atherosclerosis – a procedure known as carotid endarterectomy (CEA). By removing the atherosclerotic plaque from the affected carotid artery of these patients, CEA is beneficial by preventing subsequent ipsilateral ischemic stroke. However, it is known that patients with low to intermediate artery stenosis may still experience ischemic events, leading clinicians to consider plaque composition as an important feature of atherosclerosis. Today molecular imaging can be used for characterization, visualization and quantification of cellular and subcellular physiological processes as they take place *in vivo*; using this technology we can obtain valuable information on atherosclerotic plaque composition. Applying molecular imaging clinically to atherosclerotic disease therefore has the potential to identify atherosclerotic plaques vulnerable to rupture. This could prove to be an important tool for the selection of patients for CEA surgery in a health system increasingly focused on individualized treatment. This review focuses on current advances and future developments of *in vivo* atherosclerosis PET imaging in man.

Introduction

Atherosclerosis is a degenerative inflammatory vascular disease (Ross, 1999). It is the primary underlying cause of CVD and by causing myocardial infarction and stroke; it has become the leading cause of morbidity and mortality in the Western world today (WHO, 2012; Go et al., 2013). The economic revolution in Southeast Asia and the accelerating urbanization of China and India, combined with the prevalence of traditional CVD risk factors in particular, is expected to increase CVD incidence dramatically by 2020 (Celermajer et al., 2012). Our knowledge of the cellular and molecular mechanisms causing and aggravating atherosclerosis has increased substantially in the last several years, however, we still face serious challenges trying to discriminate the relatively benign stable atherosclerotic plaque from the high-risk (vulnerable) plaque in a clinical setting (Fleg et al., 2012; Joshi et al., 2012). The

use of ultrasound allow some qualitative evaluation of carotid plaques; however, selection criteria for surgical intervention for high-risk plaques of the internal carotid artery; carotid endarterectomy (CEA) remains largely based on the degree of carotid stenosis (Hobson et al., 2008). What is needed is a clinical tool for identification of the vulnerable plaque so that CEA is only performed on patients standing to benefit from the procedure, thereby reducing the numbers needed to treat which is currently about six to one (Chaturvedi et al., 2005). Molecular imaging has the potential as a tool for identification of the vulnerable plaque; allowing for risk stratification and individualized preventive intervention, as well as enabling clinicians to monitor the effect of medical therapy.

Molecular imaging is a technology enabling visualization of the molecular interaction and distribution of a probe (hereon referred to as a tracer) with its target or pathway in an intact biological system, i.e. *in vivo*. Existing molecular imaging

modalities comprise contrast-enhanced ultrasound, optical imaging, magnetic resonance imaging (MRI), single photon emission computed tomography (SPECT) and positron emission tomography (PET). It is the scope of this review to present current advances and potential future applications of PET for *in vivo* atherosclerotic disease management in human patients.

Pathogenesis of atherosclerosis

Atherosclerosis is a systemic artery vessel wall disease characterized by inflammation (Ross, 1999; Hansson & Libby, 2006). Originally, plaque development was subdivided into four major stages, whereas the modern perception is that of a more seamless transition over time. Initiation of plaque development is a result of endothelial dysfunction with a decrease in nitric oxide (NO) bioavailability, oxidative excess and subsequent inflammation (Endemann & Schiffrin, 2004; Vita, 2011). A pro-inflammatory state results and expression of vascular cell adhesion molecule-1 (VCAM-1) and intercellular adhesion molecule-1 (ICAM-1) by endothelial cells (ECs) initiate white blood cell recruitment (Endemann & Schiffrin, 2004). Monocytes then infiltrate the artery intima where they differentiate into macrophages and start to engulf lipids such as oxidized low-density lipoprotein (oxLDL), primarily via scavenger receptors class A, B and D, resulting in macrophage transformation into foam cells and development of a fatty streak (Libby, 2002; Rahaman et al., 2006; Ashraf & Gupta, 2011). With increased complexity of the lesion, foam cells become overwhelmed and form a necrotic core. Chemokines such as C-C motif ligand-2 (CCL-2) and monocyte chemoattractant protein-1 (MCP-1) secreted from ECs and vascular smooth muscle cells (VSMCs) stimulate a continuous influx of white blood cells into the lesion (Hansson & Libby, 2006). Foam cell remnants and necrotic debris then make up a highly thrombogenic lipid rich core and VSMCs start migrating into the lesion to form the basis of a fibrous cap by modification of the extracellular matrix. A hypoxic microenvironment stimulate the formation of microvessels from the *vasa vasorum* forming a highly immature plaque vasculature facilitating further white blood cell recruitment and haemorrhagic episodes due to microvessel immaturity (Virmani et al., 2005). The fulminant plaque may then protrude into the arterial lumen increasing the risk of organ ischemic events distal to the plaque, see Fig. 2. An acellular plaque with a large lipid core separated from the blood by a thin fibrous cap may rupture and lead to myocardial infarction or stroke and is therefore by definition a vulnerable plaque (Finn et al., 2010).

Positron emission tomography

The PET is a medical imaging technique based on the detection of radioactive decay from positron emitting radionuclides (β^+ decay). The radionuclide coupled tracer is usually administered intravenously when clinically used. The tracer is

designed to target a specific biochemical or pharmacological interaction *in vivo*, which can then be visualized in 3D following computer reconstruction, qua the associated radioactive decay which is recorded by the PET scanner (Cherry & Dahlbom, 2004). By drawing regions of interest (ROIs) on reconstructed imaging data the quantity of tracer uptake can be calculated for that region. The first *in vivo* detection of annihilation radiation (see below) as we know it today was performed in two dogs in 1975 using a prototype positron emission tomograph (Phelps et al., 1975; Ter-Pogossian et al., 1975). The positron is essentially a positive electron (e^+) ejected from the isotope nucleus with a kinetic energy in the range of a few mega-electron volt (MeV). As the positron travels through tissue, the kinetic energy is deposited by multiple direction changing interactions with tissue electrons prior to uniting with an electron (e^-) to undergo annihilation whereby the mass of the positron and an electron is converted into electromagnetic energy. The reaction produces two photons with the energy of 511 kilo-electron volt (keV) emitted back to back.

The PET scanner detects annihilation photons that escape the body. The detection system is configured so that opposite detectors is coupled to form a coincidence circuit in which the back to back emitted photons can be detected within a specified time window. The volume between the detector pairs where the coincidence detection takes place is called the line of response (LOR) and is made up by voxels each representing a 3D volume in space. Detection of thousands and thousands of these events at different angles and radial offsets followed by extensive computer analysis allows reconstruction of 3D images (Phelps et al., 1975; Cherry & Dahlbom, 2004).

A particular challenge to clinical PET imaging is the imaging of small structures as that of the vessel wall in atherosclerotic disease. The inherent 'blurring' of PET images is due to the finite spatial resolution of the system of which two fundamental limitations are of paramount importance; acollinearity and positron range (Cherry & Dahlbom, 2004; Moses, 2011). Of these factors only positron range can be affected and only by either selecting an alternate parent isotope or by using a powerful magnetic field to affect positron trajectory thereby decreasing positron range. Both options present great challenges in either chemical synthesis effort, or high equipment cost and are therefore considered impractical (Moses, 2011). However, the recent emergence of the first combined clinical PET/MRI scanners may prove an exception to at least part of this consensus (Schlemmer et al., 2008). Another important consideration when imaging small structures is the partial volume effect which describes how a small lesion with high tracer uptake in a low tracer background will result in the signal being spread out. This spill-out of signal from the lesion is also true for signal spilling back in from the background making the partial volume effect very hard to predict and compensate. In a small lesion this interprets to a lesser maximal value of lesion tracer uptake than the actual maximum value tracer uptake as well as an apparent larger lesion size (Cherry &

Dahlbom, 2004; Soret et al., 2007). It is important to understand that partial volume effect does not cause signal loss, but that it does cause signal displacement (Soret et al., 2007).

Annihilation photons are likely to experience either attenuation or scatter events predominantly by Compton interactions in the tissue and the result is the removal of the annihilation photon from the original LOR. Recent advances have led to the implementation of analytical models correcting for single scatter events, by single scatter scaling (SSS), which is a reasonable approximation of total scatter when compared with modelling of events of second or higher order of scatter (Polycarpou et al., 2011). With the introduction of the first clinical hybrid PET/CT scanners (Beyer et al., 2000), attenuation correction can be performed by direct measurement using the CT modality to calculate a map of attenuation coefficients, of the patient, which is subsequently used to correct PET emission data (Burger et al., 2002).

Although the limited spatial resolution of PET is a major disadvantage when imaging small structures such as the vessel wall this can be complemented by co-registration with either CT or MRI, whereby detailed anatomical information can be combined with the PET imaging modality to locate precisely the anatomical distribution of tracer uptake and ease the drawing of ROIs (Beyer et al., 2000; Von Schulthess et al., 2006; Schlemmer et al., 2008). With acollinearity and positron range being fundamental limitations, the best intrinsic spatial resolution of full body clinical PET scanners achievable is just below 3 mm at the centre field of view (Moses, 2011); however, using algorithms to modify the point spread function (PSF) of the scanner a resolution as good as 2 mm is practically achievable (Panin et al., 2006; Levin et al., 2012).

PET tracers in atherosclerosis

When considering the bulk of PET tracer use there are basically two types of tracers clinically used; 2-[¹⁸F]-fluoro-2-deoxy-D-glucose (¹⁸F-FDG) and the more recently introduced non-¹⁸F-FDG tracers. At the Department of Nuclear Medicine, Clinical Physiology & PET, Rigshospitalet in Copenhagen approximately 88% of all PET imaging in the years 2004–2012 was performed using ¹⁸F-FDG (internal communication). Being a university hospital, Rigshospitalet has a high research activity and a comparable conventional PET facility would perform approximately 95–100% of all PET imaging using ¹⁸F-FDG. Therefore, we will discuss the research of atherosclerosis according to these two tracer types. Important milestones and novel research areas of each type are summarized in Tables 1 and 2 respectively.

¹⁸F-FDG

¹⁸F-FDG is the workhorse among the PET tracers. It is a glucose analogue with the positron emitter ¹⁸F ($t_{1/2} = 110$ min) substituted for the OH-group in the second position of the carbon backbone of D-glucose. A reproducible synthesis

method of ¹⁸F-FDG was first reported in the late 1970s (Gallagher et al., 1977; Ido et al., 1978); however, as early as 1976, the first two human volunteers at the University of Pennsylvania were administered ¹⁸F-FDG. ¹⁸F-FDG enables visualization of tissues with an elevated level of glycolysis by a process of metabolic trapping (Gallagher et al., 1978), Fig. 1.

In 1977 the first ¹⁸F-FDG scan was reported using a human subject. The images were recorded of the cerebrum, however, a non-PET scanner was used (Reivich et al., 1977). The discovery that a high metabolic demand for glucose was a key requirement of cancer cells was discovered as early as the 1920s by Otto Warburg and was aptly referred to as the Warburg effect ever since (Warburg et al., 1924). Today the heritage of Otto Warburg is carried on by ¹⁸F-FDG as the main PET tracer of choice in standalone PET and hybrid PET/CT imaging in cancer patient management (Von Schulthess et al., 2006; Czernin et al., 2010a). It has come to the attention of clinicians and researchers in turn that accumulation of ¹⁸F-FDG is linked not only to cancer, but to benign and more generalized pathology as well. Accordingly, ¹⁸F-FDG uptake is expected to be noticeable during the course of atherogenesis in which inflammatory activity and thereby glycolysis is high (Vallabhajosula & Fuster, 1997; Shreve et al., 1999).

In 2001 this awareness led to the first retrospective report of ¹⁸F-FDG uptake in the large arteries of cancer patients (Yun et al., 2001) and this was soon followed by the first prospective study designed to evaluate atherosclerotic disease using ¹⁸F-FDG PET/CT in man (Rudd et al., 2002). The latter study also used an elegant approach with tritiated deoxyglucose (an *in vitro* analogue of ¹⁸F-FDG) and autoradiography to demonstrate that activity accumulated in macrophage rich areas of atherosclerotic plaques. This made it plausible that macrophages were responsible for the ¹⁸F-FDG-uptake seen by PET/CT *in vivo*, see Fig. 2, an observation very much in line with the emerging consensus that atherosclerosis is an inflammatory disease (Ross, 1999). As a natural consequence of this work, the first study to seek to quantitate lesion macrophages by immunohistochemistry (% CD68 staining) to *in vivo* ¹⁸F-FDG uptake; target to background ratio (TBR) found a good correlation between the two ($r = 0.70$; $P < 0.0001$) when comparing sections of internal carotid lesions to corresponding imaging data obtained prior to CEA (Tawakol et al., 2006). An even better correlation was found when comparing mean ¹⁸F-FDG uptake to mean lesion (% CD68 staining) inflammation ($r = 0.85$; $P < 0.0001$) (Tawakol et al., 2006).

This was later corroborated in two studies using patient subsets from the prior study to correlate % CD68 staining with TBR (Fifer et al., 2011; Figueroa et al., 2012). The earlier of those two studies made the comparison indirectly and was a cross-sectional study of retrospective nature. Although highly significant and comparable correlations were found in the three studies, the question of timing from the ¹⁸F-FDG PET scan to CEA could be raised as patients went for up to a month before having their plaque removed. That question was addressed when it was determined that ¹⁸F-FDG PET scans

Table 1 Milestones; In vivo ^{18}F -FDG-uptake in human atherosclerosis using PET.

Target	Modality	Study type	Notes	Reference
	Standalone PET	Retrospective study of cancer patients	First report on ^{18}F -FDG-uptake in arteries	Yun et al. (2001)
	Sequential PET/CT with retrospective imaging alignment	Prospective study (first)	First study specifically of atherosclerosis in humans using PET/CT	Rudd et al. (2002)
	Hybrid PET/CT	Retrospective study of cancer patients	First report using true hybrid PET/CT to study atherosclerosis	Tatsumi et al. (2003)
M Φ (CD68), immunohistochemistry	Sequential PET/CT and PET/MRI with retrospective imaging alignment	Prospective and correlational to cell type (M Φ)	First noninvasive study to assess inflammation by M Φ infiltration quantitatively	Tawakol et al. (2006)
Drug intervention, Simvastatin	Sequential PET/CT with retrospective imaging alignment	Prospective study of patients screened for cancer	First interventional study, attenuation of ^{18}F -FDG-uptake found	Tahara et al. (2006)
PET reproducibility in atherosclerosis	Hybrid PET/CT	Prospective study of patients with vascular disease	Very good interscan variability for the internal carotid artery: 0.90; CI: 0.68–0.97	Rudd et al. (2007)
CD68, cathepsin K, MMP-9 and IL-18 gene expression	Hybrid PET/CT	Prospective study of patients receiving surgery (CEA) for atherosclerosis	First study of the molecular pathology of atherosclerosis	Graebe et al. (2009)
Angiogenesis; gene expression of $\alpha_v\beta_3$, CD34 and VEGF	Hybrid PET/CT	Prospective study of patients receiving surgery (CEA) for atherosclerosis	First study of angiogenesis using ^{18}F -FDG	Pedersen et al. (2012)
Hypoxia; gene expression of HIF-1 α	Hybrid PET/CT	Prospective study of patients receiving surgery (CEA) for atherosclerosis	First study of hypoxia using ^{18}F -FDG	Pedersen et al. (2013)
Comparison of PET/MRI to PET/CT	Hybrid PET/MRI	Feasibility of simulta-neous PET/MRI for ^{18}F -FDG imaging of carotid arteries	First PET/MRI in carotid arteries	Ripa et al. (2013)

$\alpha_v\beta_3$, integrin dimer consisting of integrin α_v and integrin β_3 ; CD34, cluster of differentiation 34; CD68, cluster of differentiation 68 – a macrophage marker; CEA, carotid endarterectomy; CI, confidence interval (95%); CT, computed tomography; ^{18}F -FDG, 2-[^{18}F]-fluoro-2-deoxy-D-glucose; HIF-1 α , hypoxia inducible factor-1 α ; IL-18, interleukin 18; M Φ , macrophages; MMP-9, matrix metalloproteinase-9; MRI, magnetic resonance imaging; PET, positron emission tomography; VEGF, vascular endothelial growth factor.

Table 2 Novel PET tracers for human use: Potential in atherosclerosis risk stratification?

Target	Modality	Study type	Notes	Reference
Active calcification using ^{18}F -NaF	Hybrid PET/CT	Retrospective study of cancer patients	First report and feasibility study of atherosclerosis in different arterial vascular beds using ^{18}F -NaF	Derlin et al. (2010)
M Φ activity (SSTR $_2$)	Hybrid PET/CT	Retrospective study of cancer patients	First study of M Φ activity in atherosclerosis using the tracer ^{68}Ga -DOTATATE	Rominger et al. (2010)
M Φ activity (SSTR $_2$) and glycolysis	Hybrid PET/CT	Retrospective study of cancer patients	First comparison of ^{18}F -FDG and ^{68}Ga -DOTATATE in atherosclerotic disease	Li et al. (2012)
Hypoxia	Standalone PET	Prospective study of cancer patients	First study of hypoxia using ^{18}F -FMISO uptake in cancer patients	Valk et al. (1992)
Hypoxia	Standalone PET	Prospective study of cancer patients	First study of hypoxia using ^{62}Cu -ATSM uptake in cancer patients	Takahashi et al. (2000)
Angiogenesis ($\alpha_v\beta_3$)	Standalone PET	Biodistribution and pharmacokinetics study	First study of angiogenesis using ^{18}F -Galacto-RGD in cancer patients	Beer et al. (2005)

$\alpha_v\beta_3$, integrin receptor dimer $\alpha_v\beta_3$; CT, computed tomography; ^{62}Cu -ATSM, ^{62}Cu -diacetyl-bis(N^4 -methyl-thiosemicarbazone); ^{18}F -FDG, 2-[^{18}F]-fluoro-2-deoxy-D-glucose; ^{18}F -FMISO, ^{18}F -fluoromisonidazole; ^{18}F -NaF, ^{18}F -sodium fluoride; ^{68}Ga -DOTATATE, ^{68}Ga -[1,4,7,10-tetraazacyclododecane- N,N',N'',N''' -tetraacetic acid]-Phe 1 , Tyr 3 -octreotate; M Φ , macrophages; PET, positron emission tomography; SSTR $_2$, somatostatin receptor subtype 2.

performed 2 weeks apart on the same cohort of patients exhibited an interscan variability (0.90, 95% confidence interval; CI: 0.68–0.97), inter-observer agreement (0.97; CI: 0.89–0.99) and finally intra-observer agreement (0.95; CI: 0.89–0.99) for the carotid arteries (Rudd et al., 2007). The latter study was followed by a set of recommendations for ^{18}F -FDG PET/CT imaging in human subjects with atherosclerosis and a demonstration of even better performance in a study with a comparative design, but including more different

vascular beds (Rudd et al., 2008). The low numbers of patients included in these two studies is a limitation (11 and 19 patients, respectively) and two retrospective cancer studies have quite clearly demonstrated that long term ^{18}F -FDG uptake in major arterial segments change in a large proportion of re-evaluated patients over the course of several months (Ben-Haim et al., 2006; Wasselius et al., 2009a). However, if time from the initial PET scan to CEA can be reduced to match the former studies (Rudd et al., 2007, 2008) or perhaps even shorter, the validity of the correlation between the imaging modality and the subsequent tissue analysis should, theoretically, pose no problem.

The thickness of the vessel walls of the large arteries are on the edge of the resolution of the best standalone PET systems today. Therefore, the emergence of true hybrid PET/CT scanners (Beyer et al., 2000) represented a leap in molecular imaging, which was quickly evaluated to establish its potential in human atherosclerosis research (Tatsumi et al., 2003). The first prospectively designed study to use optimal post-injection scan times (3 h) in combination with almost immediate plaque recovery came from our group in 2009. We demonstrated a correlation between molecular pathology (gene

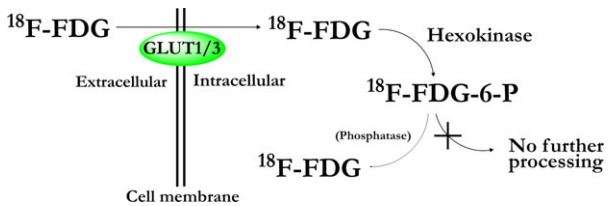


Figure 1 Metabolic trapping of ^{18}F -FDG: The inflammatory active cells take up ^{18}F -FDG via GLUT1/3. Phosphorylation by hexokinase in the cytosol yields ^{18}F -FDG-6-Phosphate which cannot be further processed by the metabolic machinery of the cell, effectively trapping ^{18}F -FDG. The slim arrow depicts the reciprocal reaction which does occur but is negligible. ^{18}F -FDG, 2-[^{18}F]-fluoro-2-deoxy-D-glucose.

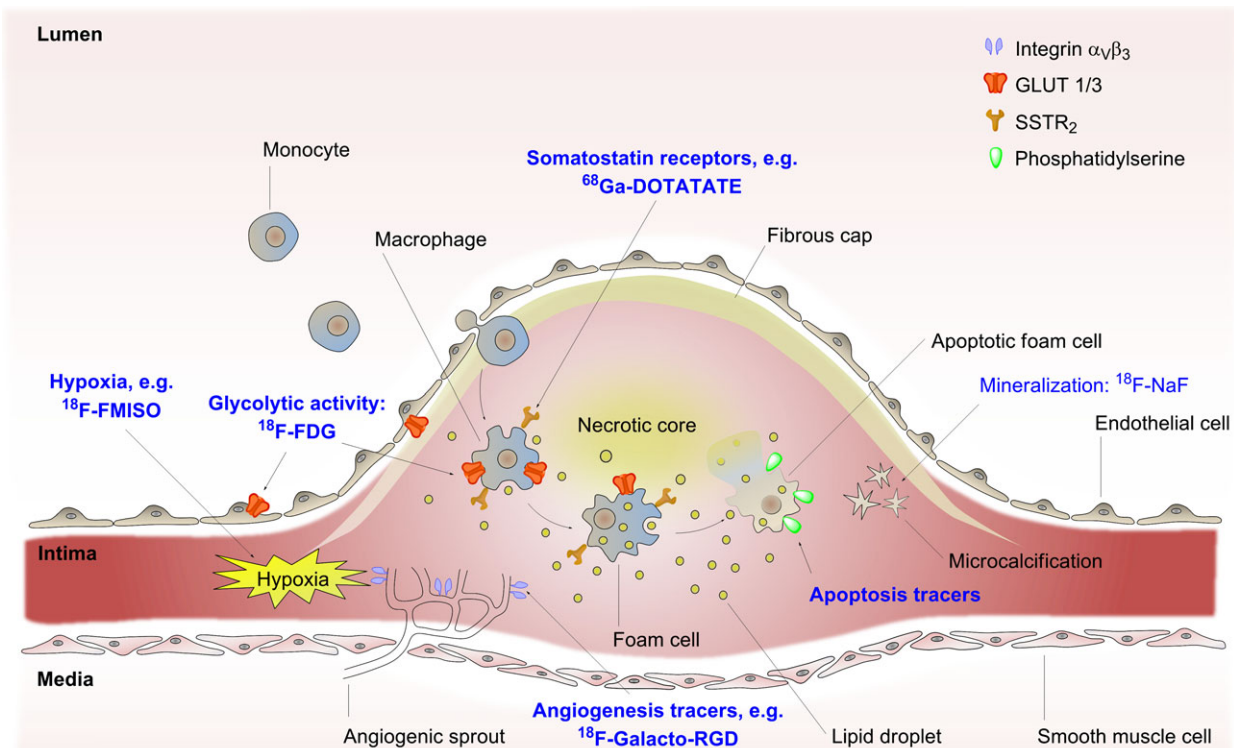


Figure 2 Atherosclerosis and molecular imaging: The vulnerable atherosclerotic plaque protrudes into the vessel lumen as a result of progressive inflammation of the vessel wall intima. Monocytes are continuously recruited from the blood and into the intima where they differentiate to macrophages and become foam cells due to lipid ingestion. Eventually, foam cells are overcome and become apoptotic amassing to a lipid rich necrotic core which is covered by a thin fibrous cap. Expansion of the intima leads to hypoxia which drives angiogenesis whereby new blood vessels sprout from the vasa vasorum in the vessel wall media. PET-tracers are depicted in blue and arrows point to their respective molecular targets. Integrin $\alpha_v\beta_3$, integrin receptor dimer $\alpha_v\beta_3$; ^{18}F -FDG, 2-[^{18}F]-fluoro-2-deoxy-D-glucose; ^{18}F -FMISO, ^{18}F -fluoromisonidazole; ^{18}F -NaF, ^{18}F -sodium fluoride; ^{68}Ga -DOTATATE, ^{68}Ga -[1,4,7,10-tetraazacyclododecane-N,N',N'',N'''-tetraacetic acid]-Phe¹, Tyr³-octreotate; GLUT, glucose transporter; PET, positron emission tomography; SSTR₂, somatostatin receptor subtype 2.

expression) and ^{18}F -FDG-uptake using hybrid PET/CT with a focus on molecular markers of inflammation and vulnerability (Graebe et al., 2009). In that study CEA was performed the day after the ^{18}F -FDG PET/CT scan and the correlation between ^{18}F -FDG-uptake and gene expression of the macrophage marker CD68 ($r = 0.71$; $P = 0.02$ and $n = 10$) was comparable with the first immunohistochemical findings on a per-patient level (Tawakol et al., 2006). Further investigations which included more patients reproduced the findings regarding CD68 ($r = 0.38$; $P < 0.0001$ and $n = 17$) using a slice-by-slice approach of each lesion for comparison with ^{18}F -FDG uptake (Pedersen et al., 2010).

Atherogenesis leads to remodelling and thickening of the vessel wall intima which may precipitate hypoxia and lead to angiogenesis as a compensatory measure (Ribatti et al., 2008), Fig. 2. Evidence of hypoxia was first produced in an elegant non-imaging study (Sluimer et al., 2008) and this was corroborated by an *in vitro* study using an ^{18}F -FDG-analog to produce evidence that hypoxia, not inflammation, increased glucose-uptake by macrophages *per se* (Folco et al., 2011). The first study directly linking the marker of hypoxia; hypoxia inducible factor-1 α (HIF-1 α) to ^{18}F -FDG-uptake *in vivo* was recently published by our group (Pedersen et al., 2013). So far a single study has explored the association between neoangiogenesis, by gene expression of the integrin dimer $\alpha_v\beta_3$ and ^{18}F -FDG-uptake in man, however, no correlation was found (Pedersen et al., 2012). Finally, a brand new study introduced demonstrated the feasibility of simultaneous hybrid PET/MRI of the carotid arteries using ^{18}F -FDG (Ripa et al., 2013).

The promise of ^{18}F -FDG PET as a method to monitor medical intervention in atherosclerosis was explored in the first interventional study using the HMG-CoA reductase inhibitor simvastatin (in a dynamic dose regime; 5–20 mg day $^{-1}$) in addition to dietary management compared with a purely dietary management group (Tahara et al., 2006). That study found that simvastatin alone attenuated plaque ^{18}F -FDG-uptake in the thoracic aorta and/or carotid arteries, and that this correlated with high-density lipoprotein cholesterol (HDL-C) elevation. A more recent study using atorvastatin in low (5 mg day $^{-1}$) and high (20 mg day $^{-1}$) dose found that a reduction in ^{18}F -FDG-uptake in the ascending aorta and the femoral artery was associated with low-density lipoprotein cholesterol (LDL-C) reduction in both groups, however, only the high dose of atorvastatin led to significant attenuation of the ^{18}F -FDG signal when compared with the baseline scan (Ishii et al., 2010). Furthermore, no difference in ^{18}F -FDG-uptake between the treatment groups was found, and therefore any dose-response relationship could not be elucidated. The latest statin-based interventional study used atorvastatin (40 mg day $^{-1}$) to treat previously statin free (1 year) subjects with confirmed significant atherosclerosis of at least one vascular territory (Wu et al., 2012). Seven different arterial segments were measured to assess ^{18}F -FDG-uptake and again a significant reduction of ^{18}F -FDG-uptake was found with treatment. In agreement with the earlier study (Ishii et al., 2010)

circulating LDL-C was lowered but in contrast to the first interventional study (Tahara et al., 2006) HDL-C was now found to be significantly reduced (Wu et al., 2012). No change, however, was seen in the coronary artery calcium (CAC) score or various adipose fat volume measurements. Earlier findings suggested that statin treatment reduce ^{18}F -FDG active plaques and with it calcified late-stage plaque burden which support the notion that ^{18}F -FDG accumulation represents a transient inflammatory state culminating in a calcified non-reversible endpoint (Wasselius et al., 2009b).

Very recently ^{18}F -FDG PET has been introduced in clinical drug trials with TBR measurements as primary endpoint of an index vessel selected on the basis of the highest average maximum TBR before and after treatment with losmapimod (a p38 mitogen-activated protein kinase inhibitor) as add-on therapy to statins. Significant attenuation of ^{18}F -FDG uptake in active sites of inflammation was found, however, not upon evaluation of the vessels using an all-segment TBR approach (Elkhwad et al., 2012). The dal-PLAQUE study used dalcetrapib (a cholesteryl ester transfer protein modulator) as add-on therapy to LDL lowering therapy. It was found that an increase in HDL-C was associated with a decrease in TBR of most-diseased-segments of artery as well as attenuation of total vessel area; however, that effect was only recorded in the carotid arteries, not the index vessels (Fayad et al., 2011). Active sites of inflammation are the most cell rich sites of atherosclerotic plaques with macrophages and vascular smooth muscle cells (VSMC) making up the bulk of the cells (Jonasson et al., 1986), we therefore suggest that any effect measured by ^{18}F -FDG PET would most likely be associated with such characteristics.

With careful consideration of sample size; what is cumulatively learned by these interventional studies is that statin treatment reduces ^{18}F -FDG-uptake in atherosclerotic plaques whether it be reported by the mean/maximal standardized uptake value (SUV_{mean} , SUV_{max}) (Tahara et al., 2006; Wasselius et al., 2009b) or the target to background (TBR) model of ^{18}F -FDG accumulation (Ishii et al., 2010; Wu et al., 2012). Interventional studies using novel drugs demonstrate that ^{18}F -FDG PET can be used to assess drug effects on plaques in a clinical setting (Fayad et al., 2011; Elkhwad et al., 2012). The case is made for large cohort event-driven prospective studies to further elucidate the anti-inflammatory effect of statins as well as novel drugs for treatment of atherosclerosis and the eligibility of ^{18}F -FDG-PET as a surrogate endpoint to monitor such non-invasive therapy.

Non-FDG PET-tracers in atherosclerosis imaging

From the diversity of studies presented, it becomes apparent that for its excellent properties ^{18}F -FDG has one major drawback; its lack of specificity. As all living cells can utilize glucose we need a tracer that specifically targets the cell-mediated key molecular processes associated with the vulnerable

atherosclerotic plaque. Most prominent of these targets are macrophage infiltration, calcification, apoptosis, hypoxia and neoangiogenesis of the intima/media (Ross, 1999; Tawakol et al., 2006; Ribatti et al., 2008; Sluimer et al., 2008; Dweck et al., 2012).

¹⁸F-NaF

One feature in atherogenesis is localized 'spotty' calcification which is thought to promote plaque vulnerability (Motoyama et al., 2007). The tracer sodium [¹⁸F]-fluoride ¹⁸F-NaF was originally developed and introduced for bone scintigraphy in 1962 (Blau et al., 1962) but has re-emerged recently with the introduction of PET, see Fig. 2. ¹⁸F-NaF is deposited by chemisorption onto hydroxyapatite (Czernin et al., 2010b) and that infers hydroxyapatite presence within the atherosclerotic lesion itself. Mineralization of the artery wall can be initiated by VSMCs responding to stress by oxidized lipids (Watson et al., 1994; Yan et al., 2011) as well as inflammation and macrophage accumulation which coincide with osteogenic activity (Aikawa et al., 2007). It is beyond the scope of this review to extensively cover the background of osteogenesis in atherosclerosis; which has excellently been discussed previously (Doherty et al., 2003; Demer & Tintut, 2011). Using hybrid PET/CT and a retrospective approach it was recently described how ¹⁸F-NaF accumulated in atheroma of the aorta, iliac, femoral and carotid arteries (Derlin et al., 2010, 2011); however, also that coincidental ¹⁸F-NaF and ¹⁸F-FDG uptake (14 of 215 lesions; 6.5%) is rare (Derlin et al., 2011). This could be due to different lesion properties, e.g. inflammation versus calcification, although it cannot be ruled out that time between ¹⁸F-NaF and ¹⁸F-FDG scans may have influenced this result (Derlin et al., 2011). A recent study scanned the patients 1 day apart and found a modest correlation ($r^2 = 0.171$, $P < 0.001$) between ¹⁸F-NaF and ¹⁸F-FDG uptake in calcific aortic valvular disease (Dweck et al., 2013). Although this seems to support the initial observation of poorly overlapping uptake patterns of ¹⁸F-NaF and ¹⁸F-FDG, the studies are not directly comparable and data are not identically presented. Contrary to ¹⁸F-FDG, ¹⁸F-NaF specifically targets bone and bone turnover and we have no reason to believe that uptake of these two tracers should perfectly coincide. This lack of tracer uptake co-localization earlier led investigators to hypothesize that it was a reflection of differences in disease stage (Derlin et al., 2011).

In another study ¹⁸F-NaF uptake was found to be associated with major adverse cardiovascular events as well as an increase in Framingham risk prediction score (Dweck et al., 2012). More importantly 41% of patients with CAC score >1000 had no significant ¹⁸F-NaF uptake and that adds weight to the hypothesis that only metabolically active calcific plaques are imaged by ¹⁸F-NaF (Dweck et al., 2012), i.e. late plaques developing an increasingly vulnerable phenotype. However, *bona fide* histological validation of this hypothesis is still lacking. With careful consideration of the research we find it justified to assume that ¹⁸F-NaF PET scan adds independent information to what is

learned from an ¹⁸F-FDG PET scan alone. A very recent publication produced evidence that plaque calcification followed focal inflammation in the same arterial location as detected by ¹⁸F-FDG PET at an earlier time point (Abdelbaky et al., 2013). Based on the newest data, further assessment of ¹⁸F-NaF PET in atherosclerosis should certainly be warranted, however, the first prospective studies are still to be seen.

⁶⁸Ga-DOTATATE

The inflammatory active atherosclerotic lesion is continuously infiltrated by blood monocytes that differentiate into macrophages which eventually become lipid loaded foam cells (Ross, 1999). The association between ¹⁸F-FDG uptake and macrophages has been substantiated earlier (Rudd et al., 2002; Tawakol et al., 2006), however, by targeting the somatostatin receptor subtype 2 (SSTR₂) expressed by macrophages (Dalm et al., 2003; Armani et al., 2007), it should be possible to obtain higher specificity than what ¹⁸F-FDG PET offers (Fig. 2) and potentially reveal all states in plaque development where macrophages are abundant. The somatostatin receptor ligand ⁶⁸Ga-[1,4,7,10-tetraazacyclododecane-N,N',N'',N'''-tetraacetic acid]-Phe¹,Tyr³-octreotate (DOTATATE) has high affinity for SSTR₂ (Breeman et al., 2005) and can be used in combination with ¹⁸F-FDG for imaging and evaluation of neuroendocrine tumors by clinical PET (Kayani et al., 2008). The potential for imaging macrophages in atherosclerosis was first explored in a study comparing ⁶⁸Ga-DOTATATE uptake in the coronary arteries with presence of calcified plaques and risk factors for cardiovascular disease (Rominger et al., 2010). Male sex and prior vascular events correlated with ⁶⁸Ga-DOTATATE uptake (TBR) and a correlation with calcified plaques was also found ($R = 0.34$; $P < 0.01$). However, in 14 of 25 (56%) of cases no colocalization with calcified plaques and ⁶⁸Ga-DOTATATE uptake was found, suggesting not all calcified plaques had a significant macrophage population (Rominger et al., 2010). The fact that less than half of the calcified plaques exhibited ⁶⁸Ga-DOTATATE accumulation could suggest that end-stage or 'stable' calcified plaques without active inflammation may account for the bulk of the ⁶⁸Ga-DOTATATE negative calcified plaques. It would be interesting to see what could be learned from comparison between ⁶⁸Ga-DOTATATE and ¹⁸F-NaF scans in this context. The second of the two existing studies using ⁶⁸Ga-DOTATATE so far, compared ⁶⁸Ga-DOTATATE to ¹⁸F-FDG uptake in a retrospective study of cancer patients (Li et al., 2012). The earlier findings was corroborated when ⁶⁸Ga-DOTATATE was found to correlate with calcified plaques ($R = 0.52$; $P < 0.05$), however, less than half (43%) of vascular sites with the highest focal ⁶⁸Ga-DOTATATE uptake was also ¹⁸F-FDG positive and conversely only 28% of the sites with the highest focal ¹⁸F-FDG uptake sites co-localized with ⁶⁸Ga-DOTATATE (Li et al., 2012). Clearly ⁶⁸Ga-DOTATATE and ¹⁸F-FDG are not equally distributed. As pointed out by the researchers themselves the tracer kinetics of ⁶⁸Ga-DOTATATE and ¹⁸F-FDG

could be an issue as saturation kinetics could be feature of SSTR₂ receptor imaging which was not the case when using ¹⁸F-FDG (Li et al., 2012). Another study found that proliferating human umbilical vein endothelial cells expressed SSTR subtypes 2 and 5 *in vitro* suggesting a possible role in angiogenesis (Adams et al., 2005). We know angiogenesis is an important feature of the advanced plaque and therefore we cannot rule out that ⁶⁸Ga-DOTATATE may detect more than macrophages in atherosclerosis imaging. Considering these facts, the number of included patients (*n* = 70 and *n* = 16, respectively) and the retrospective nature of these two studies, care must be taken when interpreting the results. However, the stronger correlation of ⁶⁸Ga-DOTATATE than ¹⁸F-FDG with cardiovascular risk factors encourages further investigations of the distribution differences between these two tracers. Histological validation of ⁶⁸Ga-DOTATATE uptake in the atherosclerotic plaque is a logical next step as is the elucidation of the biological significance of tracer distribution for the vulnerable plaque.

Future PET-tracer targets

As mentioned earlier perhaps the three most obvious molecular processes to target in plaque imaging is hypoxia, neoangiogenesis and apoptosis. First, hypoxia of the atherosclerotic arterial wall has been found to colocalize with accumulation of foam cells and macrophages *in vivo* in an experimental rabbit model as well as in humans (Bjornheden et al., 1999; Sluimer et al., 2008). Evidence that hypoxia increase macrophage ¹⁸F-FDG uptake has been observed (Folco et al., 2011) suggests that imaging hypoxia itself may offer an alternate approach, one that is already pursued in cancer imaging (Valk et al., 1992; Takahashi et al., 2000). Second, the vitronectin receptor $\alpha_v\beta_3$ is associated with neoangiogenesis and known to be expressed in atherosclerotic arteries (Hoshiga et al., 1995). It is recognized by and binds to the arginine-glycine-aspartic acid (RGD) motif. So far human imaging studies performed with a tracer based on RGD-ligands are scarce (Beer et al., 2005, 2006) and preclinical testing has shown promise as well (Oxboel et al., 2012; Pohle et al., 2012). Third, phosphatidylserine (PS) a cell membrane phospholipid, is externalized to the outer cell membrane during apoptosis, a key feature of the vulnerable atherosclerotic plaque (Koopman et al., 1994; Kolodgie et al., 2000). Thus targeting PS is a definite possibility and has been performed as early as 2003, however, not using PET (Van de Wiele et al., 2003). With these data in mind the first clinical PET study of atherosclerosis focusing on these key molecular processes (Fig. 2) is expected in the not too distant future.

Indications for introduction of atherosclerosis PET imaging

A significant number of patients are known to suffer acute ischemic events in the absence of significant ($\leq 50\%$) artery stenosis (Aldrovandi et al., 2012; Kovacic & Fuster, 2012).

Indications for CEA are based on ipsilateral symptomatic ischemic events distal to a carotid plaque of $\geq 70\%$ degree stenosis as determined by ultrasound. Although some qualitative information can be evaluated using modern ultrasound systems, selection of patients for CEA remains largely based on the degree of stenosis (Hobson et al., 2008). In our eyes this is an inadequate approach considering the patient cohort with non-significant carotid artery stenosis who experience acute ischemic stroke. What is needed is plaque characterization whereby plaque vulnerability can be evaluated. PET could potentially be the tool that, together with ultrasound, improves patient selection criteria thereby reducing the need to treat ratio. Recent work has indicated that CEA of symptomatic low grade carotid stenosis is safe and thus better selection criteria sensitivity are warranted and should be pursued (Ballotta et al., 2013). PET is a powerful technique with unsurpassed sensitivity and should be considered as a tool for achieving this goal.

Challenges in atherosclerosis PET imaging

Recently, the concept of the 'vulnerable patient' has been introduced (Naghavi et al., 2003a,b). First, to find a regional vulnerable internal carotid artery plaque using PET does not take into account the global status of the patient being evaluated for CEA and therefore co-morbidities characterizing the vulnerable patient could be missed in such a setup. Second, although arterial ¹⁸F-FDG uptake is highly correlated between different large artery vascular territories (Rudd et al., 2009), evaluation of ¹⁸F-FDG uptake in large versus small arteries such as the coronary and cerebral arteries is largely hampered by the significant myocardial and cerebral ¹⁸F-FDG uptake. On the other hand, CT assessment of plaque burden (calcium score) in the aorta and coronary arteries revealed a strong correlation between the two (Kim et al., 2011). This could be an indication of what should be further investigated using PET in a similar setup if technically feasible. Bearing this in mind, atherosclerosis is a systemic disease and vascular territories should be evaluated separately when clinically indicated to ensure optimal treatment. A third challenge is cost: PET scans are not inexpensive and therefore PET has been subjected to economic evaluations from early clinical implementation and proved cost effective in the management of an array of cancers (Buck et al., 2010). Accordingly, if effective in identifying vulnerable carotid plaques, the cost of an unnecessary CEA surgery clearly outperforms the cost of a PET scan several-fold not to forget the unnecessary discomfort and added risk inflicted upon the patient. Finally, a clinical ¹⁸F-FDG PET/CT scan subjects the patient to ionizing radiation. In a typical whole body scanning procedure the absorbed dose from the tracer is less than half the dose received by that from the CT modality alone (Brix et al., 2005). The unmatched sensitivity, the fact that the technique is non-invasive and quantifiable, is considered to outweigh the drawbacks when imaging human atherosclerosis (Owen et al., 2011). The focus of this review has been the potential role of PET in atherosclerotic

Table 3 Comparison of non-invasive imaging modalities for atherosclerotic plaque characterization.

	PET	MRI	CT	US
Plaque 'activity' (metabolism)	+++	+	–	+
Plaque composition	–	+++	+	++
IMT – vessel wall characteristics	–	++	–	+++
Calcification	–	+	+++	++
Sensitivity	+++	++	–	–

+++ , very good performance; ++ , intermediate performance; + , limited performance; – , not applicable; CT, computed tomography; IMT, intima-media thickness; MRI, magnetic resonance imaging; PET, positron emission tomography; US, ultrasound.

disease management. Hybrid PET/CT and PET/MRI provide complementary information to the PET modality; however, it is beyond the scope of this review to venture further into the specific advantages of each alternative imaging modality. However, some key characteristics of different important imaging modalities in plaque characterization have been summarized in Table 3.

Concluding remarks

It is perhaps not immediately intuitive, but many molecular targets are shared by cancer and atherosclerotic disease. No finer example of this was the way atherosclerosis imaging research started; with the observation that some cancer patients had an increased ^{18}F -FDG uptake in the large arteries (Yun et al., 2001). From that, as well as the other examples reviewed, it is likely that future tracer 'firsts' in atherosclerosis imaging will continue to be of retrospective nature with a foundation in cancer research. It follows that by rationally and systematically re-evaluating 'old' tracers in retrospective

studies before putting them to use in a new context, the achievements in PET-based atherosclerosis research brings hope for a better understanding of this disease on a molecular level. From what is seen in this review it is obvious that there is a continuous drive in the imaging community towards testing of existing tracers in new contexts. As important as this, there is focus on the development of new tracers for molecular imaging of atherosclerosis using PET. What knowledge is gained from the existing tracers should be applied for further development of new tracers followed by comprehensive prospective preclinical testing in animal models. Finally, promising new tracers should be introduced in small populations paving the way for full clinical implementation. In atherosclerosis research, the aim is the development of a safe clinical tool for non-invasive *in vivo* risk stratification of patients with symptomatic atherosclerotic disease. With apoptosis and new angiogenesis tracers close to clinical introduction the future for molecular imaging is rich in perspectives. The goal should be to learn as much as possible whereas improving and ideally substituting current implementations to benefit future patients in need of stratification for vascular surgery.

On a final note the first true event-driven prospective studies in atherosclerosis using molecular imaging were initiated in 2008/2009; the high-risk plaque initiative (Falk et al., 2011) and the associated BioImage study (Muntendam et al., 2010). As we are waiting for these results we should commit ourselves to continuously apply new as well as established tracers in new contexts in clinical research working towards an even brighter future for patients with atherosclerosis as well as for molecular imaging itself.

Conflict of interest

The authors have no conflicts of interest.

References

- Abdelbaky A, Corsini E, Figueroa AL, Fontanez S, Subramanian S, Ferencik M, Brady TJ, Hoffmann U, Tawakol A. Focal arterial inflammation precedes subsequent calcification in the same location: a longitudinal FDG-PET/CT Study. *Circ Cardiovasc Imaging* (2013); **6**: 747–754.
- Adams RL, Adams IP, Lindow SW, Zhong W, Atkin SL. Somatostatin receptors 2 and 5 are preferentially expressed in proliferating endothelium. *Br J Cancer* (2005); **92**: 1493–1498.
- Aikawa E, Nahrendorf M, Figueiredo JL, Swirski FK, Shtatland T, Kohler RH, Jaffer FA, Aikawa M, Weissleder R. Osteogenesis associates with inflammation in early-stage atherosclerosis evaluated by molecular imaging *in vivo*. *Circulation* (2007); **116**: 2841–2850.
- Aldrovandi A, Cademartiri F, Arduini D, Lina D, Ugo F, Maffei E, Menozzi A, Martini C, Palumbo A, Bontardelli F, Gherli T, Ruffini L, Ardissino D. Computed tomography coronary angiography in patients with acute myocardial infarction without significant coronary stenosis. *Circulation* (2012); **126**: 3000–3007.
- Armani C, Catalani E, Balbarini A, Bagnoli P, Cervia D. Expression, pharmacology, and functional role of somatostatin receptor subtypes 1 and 2 in human macrophages. *J Leukoc Biol* (2007); **81**: 845–855.
- Ashraf MZ, Gupta N. Scavenger receptors: implications in atherothrombotic disorders. *Int J Biochem Cell Biol* (2011); **43**: 697–700.
- Ballotta E, Angelini A, Mazzalai F, Piatto G, Toniato A, Baracchini C. Carotid endarterectomy for symptomatic low-grade carotid stenosis. *J Vasc Surg* (2013); doi: 10.1016/j.jvs.2013.06.079. [Epub ahead of print].
- Beer AJ, Haubner R, Goebel M, Luderschmidt S, Spilker ME, Wester HJ, Weber WA, Schwaiger M. Biodistribution and pharmacokinetics of the alpha(v)beta3-selective tracer ^{18}F -galacto-RGD in cancer patients. *J Nucl Med* (2005); **46**: 1333–1341.
- Beer AJ, Haubner R, Sarbia M, Goebel M, Luderschmidt S, Grosu AL, Schnell O, Niemeyer M, Kessler H, Wester HJ, Weber WA, Schwaiger M. Positron emission tomography using [^{18}F]Galacto-RGD identifies the level of integrin alpha(v)beta3 expression in man. *Clin Cancer Res* (2006); **12**: 3942–3949.
- Ben-Haim S, Kupzov E, Tamir A, Frenkel A, Israel O. Changing patterns of abnormal

- vascular wall F-18 fluorodeoxyglucose uptake on follow-up PET/CT studies. *J Nucl Cardiol* (2006); **13**: 791–800.
- Beyer T, Townsend DW, Brun T, Kinahan PE, Charron M, Roddy R, Jerin J, Young J, Byars L, Nutt R. A combined PET/CT scanner for clinical oncology. *J Nucl Med* (2000); **41**: 1369–1379.
- Bjornheden T, Levin M, Ewaldsson M, Wiklund O. Evidence of hypoxic areas within the arterial wall in vivo. *Arterioscler Thromb Vasc Biol* (1999); **19**: 870–876.
- Blau M, Nagler W, Bender MA. Fluorine-18: a new isotope for bone scanning. *J Nucl Med* (1962); **3**: 332–334.
- Breeman WA, de Jong M, de Blois E, Bernard BF, Konijnenberg M, Krenning EP. Radiolabelling DOTA-peptides with ⁶⁸Ga. *Eur J Nucl Med Mol Imaging* (2005); **32**: 478–485.
- Brix G, Lechel U, Glatting G, Ziegler SI, Munzing W, Muller SP, Beyer T. Radiation exposure of patients undergoing whole-body dual-modality 18F-FDG PET/CT examinations. *J Nucl Med* (2005); **46**: 608–613.
- Buck AK, Herrmann K, Stargardt T, Dechow T, Krause BJ, Schreyogg J. Economic evaluation of PET and PET/CT in oncology: evidence and methodologic approaches. *J Nucl Med* (2010); **51**: 401–412.
- Burger C, Goerres G, Schoenes S, Buck A, Lonn AH, Von Schulthess GK. PET attenuation coefficients from CT images: experimental evaluation of the transformation of CT into PET 511-keV attenuation coefficients. *Eur J Nucl Med Mol Imaging* (2002); **29**: 922–927.
- Celermajer DS, Chow CK, Marijon E, Anstey NM, Woo KS. Cardiovascular disease in the developing world: prevalences, patterns, and the potential of early disease detection. *J Am Coll Cardiol* (2012); **60**: 1207–1216.
- Chaturvedi S, Bruno A, Feasby T, Holloway R, Benavente O, Cohen SN, Cote R, Hess D, Saver J, Spence JD, Stern B, Wilterdink J. Carotid endarterectomy—an evidence-based review: report of the Therapeutics and Technology Assessment Subcommittee of the American Academy of Neurology. *Neurology* (2005); **65**: 794–801.
- Cherry SR, Dahlbom M. PET: physics, instrumentation, and scanners. In: *PET: Molecular Imaging and Its Biological Applications* (ed. M Phelps) (2004), pp. 1–125. New York: Springer-Verlag.
- Czernin J, Benz MR, Allen-Auerbach MS. PET/CT imaging: the incremental value of assessing the glucose metabolic phenotype and the structure of cancers in a single examination. *Eur J Radiol* (2010a); **73**: 470–480.
- Czernin J, Satyamurthy N, Schiepers C. deposition. *J Nucl Med* (2010b); **51**: 1826–1829.
- Dalm VA, Van Hagen PM, Van Koetsveld PM, Achilefu S, Houtsmuller AB, Pols DH, Van Der Lely AJ, Lamberts SW, Hofland LJ. Expression of somatostatin, cortistatin, and somatostatin receptors in human monocytes, macrophages, and dendritic cells. *Am J Physiol Endocrinol Metab* (2003); **285**: E344–E353.
- Demer L, Tintut Y. The roles of lipid oxidation products and receptor activator of nuclear factor- κ B signaling in atherosclerotic calcification. *Circ Res* (2011); **108**: 1482–1493.
- Derlin T, Richter U, Bannas P, Begemann P, Buchert R, Mester J, Klutmann S. Feasibility of 18F-sodium fluoride PET/CT for imaging of atherosclerotic plaque. *J Nucl Med* (2010); **51**: 862–865.
- Derlin T, Wisotzki C, Richter U, Apostolova I, Bannas P, Weber C, Mester J, Klutmann S. In vivo imaging of mineral deposition in carotid plaque using 18F-sodium fluoride PET/CT: correlation with atherogenic risk factors. *J Nucl Med* (2011); **52**: 362–368.
- Doherty TM, Asotra K, Fitzpatrick LA, Qiao JH, Wilkin DJ, Detrano RC, Dunstan CR, Shah PK, Rajavashisth TB. Calcification in atherosclerosis: bone biology and chronic inflammation at the arterial crossroads. *Proc Natl Acad Sci USA* (2003); **100**: 11201–11206.
- Dweck MR, Chow MW, Joshi NV, Williams MC, Jones C, Fletcher AM, Richardson H, White A, McKillop G, van Beek EJ, Boon NA, Rudd JH, Newby DE. Coronary arterial 18F-sodium fluoride uptake: a novel marker of plaque biology. *J Am Coll Cardiol* (2012); **59**: 1539–1548.
- Dweck MR, Khaw HJ, Sng GK, Luo EL, Baird A, Williams MC, Makiello P, Mirsadraee S, Joshi NV, van Beek EJ, Boon NA, Rudd JH, Newby DE. Aortic stenosis, atherosclerosis, and skeletal bone: is there a common link with calcification and inflammation? *Eur Heart J* (2013); **34**: 1567–1574.
- Elkhwad M, Rudd JH, Sarov-Blat L, Cai G, Wells R, Davies LC, Collier DJ, Marber MS, Choudhury RP, Fayad ZA, Tawakol A, Gleeson FV, Lepore JJ, Davis B, Willette RN, Wilkinson IB, Sprecher DL, Cheriyan J. Effects of p38 mitogen-activated protein kinase inhibition on vascular and systemic inflammation in patients with atherosclerosis. *JACC Cardiovasc Imaging* (2012); **5**: 911–922.
- Endemann DH, Schiffrin EL. Endothelial dysfunction. *J Am Soc Nephrol* (2004); **15**: 1983–1992.
- Falk E, Sillesen H, Muntendam P, Fuster V. The high-risk plaque initiative: primary prevention of atherothrombotic events in the asymptomatic population. *Curr Atheroscler Rep* (2011); **13**: 359–366.
- Fayad ZA, Mani V, Woodward M, Kallend D, Abt M, Burgess T, Fuster V, Ballantyne CM, Stein EA, Tardif JC, Rudd JH, Farkouh ME, Tawakol A. Safety and efficacy of dalcetrapib on atherosclerotic disease using novel non-invasive multimodality imaging (dal-PLAQUE): a randomised clinical trial. *Lancet* (2011); **378**: 1547–1559.
- Fifer KM, Qadir S, Subramanian S, Vijayakumar J, Figueroa AL, Truong QA, Hoffmann U, Brady TJ, Tawakol A. Positron emission tomography measurement of periodontal (18F)-fluorodeoxyglucose uptake is associated with histologically determined carotid plaque inflammation. *J Am Coll Cardiol* (2011); **57**: 971–976.
- Figueroa AL, Subramanian SS, Cury RC, Truong QA, Gardecki JA, Tearney GJ, Hoffmann U, Brady TJ, Tawakol A. Distribution of inflammation within carotid atherosclerotic plaques with high-risk morphological features: a comparison between positron emission tomography activity, plaque morphology, and histopathology. *Circ Cardiovasc Imaging* (2012); **5**: 69–77.
- Finn AV, Nakano M, Narula J, Kolodgie FD, Virmani R. Concept of vulnerable/unstable plaque. *Arterioscler Thromb Vasc Biol* (2010); **30**: 1282–1292.
- Fleg JL, Stone GW, Fayad ZA, Granada JF, Hatsukami TS, Kolodgie FD, Ohayon J, Pettigrew R, Sabatine MS, Tearney GJ, Waxman S, Domanski MJ, Srinivas PR, Narula J. Detection of high-risk atherosclerotic plaque: report of the NHLBI Working Group on current status and future directions. *JACC Cardiovasc Imaging* (2012); **5**: 941–955.
- Folco EJ, Sheikine Y, Rocha VZ, Christen T, Shvartz E, Sukhova GK, Di Carli MF, Libby P. Hypoxia but not inflammation augments glucose uptake in human macrophages: implications for imaging atherosclerosis with 18fluorine-labeled 2-deoxy-D-glucose positron emission tomography. *J Am Coll Cardiol* (2011); **58**: 603–614.
- Gallagher BM, Ansari A, Atkins H, Casella V, Christman DR, Fowler JS, Ido T, MacGregor RR, Som P, Wan CN, Wolf AP, Kuhl DE, Reivich M. Radiopharmaceuticals XXVII. 18F-labeled 2-deoxy-2-fluoro-D-glucose as a radiopharmaceutical for measuring regional myocardial glucose metabolism in vivo: tissue distribution and imaging studies in animals. *J Nucl Med* (1977); **18**: 990–996.
- Gallagher BM, Fowler JS, Guttererson NI, MacGregor RR, Wan CN, Wolf AP. Metabolic trapping as a principle of oradiopharmaceutical design: some factors responsible for the biodistribution of [18F] 2-deoxy-2-fluoro-D-glucose. *J Nucl Med* (1978); **19**: 1154–1161.

- Go AS, Mozaffarian D, Roger VL, Benjamin EJ, Berry JD, Borden WB, Bravata DM, Dai S, Ford ES, Fox CS, Franco S, Fullerton HJ, Gillespie C, Hailpern SM, Heit JA, Howard VJ, Huffman MD, Kissela BM, Kittner SJ, Lackland DT, Lichtman JH, Lisabeth LD, Magid D, Marcus GM, Marelli A, Matchar DB, McGuire DK, Mohler ER, Moy CS, Mussolino ME, Nichol G, Paynter NP, Schreiner PJ, Sorlie PD, Stein J, Turan TN, Virani SS, Wong ND, Woo D, Turner MB. Heart Disease and Stroke Statistics—2013 Update: a Report From the American Heart Association. *Circulation* (2013); **127**: e6–e245.
- Graebe M, Pedersen SF, Borgwardt L, Hojgaard L, Sillesen H, Kjaer A. Molecular pathology in vulnerable carotid plaques: correlation with [18]-fluorodeoxyglucose positron emission tomography (FDG-PET). *Eur J Vasc Endovasc Surg* (2009); **37**: 714–721.
- Hansson GK, Libby P. The immune response in atherosclerosis: a double-edged sword. *Nat Rev Immunol* (2006); **6**: 508–519.
- Hobson RW, Mackey WC, Ascher E, Murad MH, Calligaro KD, Comerota AJ, Montori VM, Eskandari MK, Massop DW, Bush RL, Lal BK, Perler BA. Management of atherosclerotic carotid artery disease: clinical practice guidelines of the Society for Vascular Surgery. *J Vasc Surg* (2008); **48**: 480–486.
- Hoshiga M, Alpers CE, Smith LL, Giachelli CM, Schwartz SM. Alpha-v beta-3 integrin expression in normal and atherosclerotic artery. *Circ Res* (1995); **77**: 1129–1135.
- Ido T, Wan CN, Casella V, Fowler JS, Wolf AP. Labeled 2-deoxy-D-glucose analogs. 18F-labeled 2-deoxy-2-fluoro-D-glucose, 2-deoxy-2-fluoro-D-mannose and 14C-2-deoxy-2-fluoro-D-glucose. *J Labelled Compd Radiopharm* (1978); **14**: 175–183.
- Ishii H, Nishio M, Takahashi H, Aoyama T, Tanaka M, Toriyama T, Tamaki T, Yoshikawa D, Hayashi M, Amano T, Matsubara T, Murohara T. Comparison of atorvastatin 5 and 20 mg/d for reducing F-18 fluorodeoxyglucose uptake in atherosclerotic plaques on positron emission tomography/computed tomography: a randomized, investigator-blinded, open-label, 6-month study in Japanese adults scheduled for percutaneous coronary intervention. *Clin Ther* (2010); **32**: 2337–2347.
- Jonasson L, Holm J, Skalli O, Bondjers G, Hansson GK. Regional accumulations of T cells, macrophages, and smooth muscle cells in the human atherosclerotic plaque. *Arteriosclerosis* (1986); **6**: 131–138.
- Joshi FR, Lindsay AC, Obaid DR, Falk E, Rudd JH. Non-invasive imaging of atherosclerosis. *Eur Heart J Cardiovasc Imaging* (2012); **13**: 205–218.
- Kayani I, Bomanji JB, Groves A, Conway G, Gacinovic S, Win T, Dickson J, Caplin M, Ell PJ. Functional imaging of neuroendocrine tumors with combined PET/CT using 68 Ga-DOTATATE (DOTA-DPhe1, Tyr3-octreotate) and 18F-FDG. *Cancer* (2008); **112**: 2447–2455.
- Kim EJ, Yong HS, Seo HS, Lim SY, Kim SW, Kim MN, Kim YK, Poddar KL, Ramasamy S, Na JO, Choi CU, Lim HE, Kim JW, Kim SH, Lee EM, Rha SW, Park CG, Oh DJ. Association between aortic calcification and stable obstructive coronary artery disease. *Int J Cardiol* (2011); **153**: 192–195.
- Kolodgie FD, Narula J, Burke AP, Haider N, Farb A, Hui-Liang Y, Smialek J, Virmani R. Localization of apoptotic macrophages at the site of plaque rupture in sudden coronary death. *Am J Pathol* (2000); **157**: 1259–1268.
- Koopman G, Reutelingsperger CP, Kuijten GA, Keehnen RM, Pals ST, van Oers MH. Annexin V for flow cytometric detection of phosphatidylserine expression on B cells undergoing apoptosis. *Blood* (1994); **84**: 1415–1420.
- Kovacic JC, Fuster V. Smoking gun theory: angiographically normal or mild coronary plaque as a cause of myocardial infarction. *Circulation* (2012); **126**: 2918–2920.
- Levin KT, Hogild KS, Vinter OO, Aznar M, Andersen FL. Innovations in PET/CT. *Q J Nucl Med Mol Imaging* (2012); **56**: 268–279.
- Li X, Samnick S, Lapa C, Israel I, Buck AK, Kreissl MC, Bauer W. 68 Ga-DOTATATE PET/CT for the detection of inflammation of large arteries: correlation with 18F-FDG, calcium burden and risk factors. *EJNMMI Res* (2012); **2**: 52.
- Libby P. Inflammation in atherosclerosis. *Nature* (2002); **420**: 868–874.
- Moses WW. Fundamental Limits of Spatial Resolution in PET. *Nucl Instrum Methods Phys Res A* (2011); **648**(Suppl. 1): S236–S240.
- Motoyama S, Kondo T, Sarai M, Sugiura A, Harigaya H, Sato T, Inoue K, Okumura M, Ishii J, Anno H, Virmani R, Ozaki Y, Hishida H, Narula J. Multislice computed tomographic characteristics of coronary lesions in acute coronary syndromes. *J Am Coll Cardiol* (2007); **50**: 319–326.
- Muntendam P, McCall C, Sanz J, Falk E, Fuster V. The BioImage Study: novel approaches to risk assessment in the primary prevention of atherosclerotic cardiovascular disease—study design and objectives. *Am Heart J* (2010); **160**: 49–57.
- Naghavi M, Libby P, Falk E, Casscells SW, Litovsky S, Rumberger J, Badimon JJ, Stefanadis C, Moreno P, Pasterkamp G, Fayad Z, Stone PH, Waxman S, Raggi P, Madjid M, Zarrabi A, Burke A, Yuan C, Fitzgerald PJ, Siscovick DS, de Korte CL, Aikawa M, Airaksinen KE, Assmann G, Becker CR, Chesebro JH, Farb A, Galis ZS, Jackson C, Jang IK, Koenig W, Lodder RA, March K, Demirovic J, Navab M, Priori SG, Reekter MD, Bahr R, Grundy SM, Mehran R, Colombo A, Boerwinkle E, Ballantyne C, Insull W Jr, Schwartz RS, Vogel R, Serruys PW, Hansson GK, Faxon DP, Kaul S, Drexler H, Greenland P, Muller JE, Virmani R, Ridker PM, Zipes DP, Shah PK, Willerson JT. From vulnerable plaque to vulnerable patient: a call for new definitions and risk assessment strategies: Part II. *Circulation* (2003a); **108**: 1772–1778.
- Naghavi M, Libby P, Falk E, Casscells SW, Litovsky S, Rumberger J, Badimon JJ, Stefanadis C, Moreno P, Pasterkamp G, Fayad Z, Stone PH, Waxman S, Raggi P, Madjid M, Zarrabi A, Burke A, Yuan C, Fitzgerald PJ, Siscovick DS, de Korte CL, Aikawa M, Juhani Airaksinen KE, Assmann G, Becker CR, Chesebro JH, Farb A, Galis ZS, Jackson C, Jang IK, Koenig W, Lodder RA, March K, Demirovic J, Navab M, Priori SG, Reekter MD, Bahr R, Grundy SM, Mehran R, Colombo A, Boerwinkle E, Ballantyne C, Insull W Jr, Schwartz RS, Vogel R, Serruys PW, Hansson GK, Faxon DP, Kaul S, Drexler H, Greenland P, Muller JE, Virmani R, Ridker PM, Zipes DP, Shah PK, Willerson JT. From vulnerable plaque to vulnerable patient: a call for new definitions and risk assessment strategies: Part I. *Circulation* (2003b); **108**: 1664–1672.
- Owen DR, Lindsay AC, Choudhury RP, Fayad ZA. Imaging of atherosclerosis. *Annu Rev Med* (2011); **62**: 25–40.
- Oxboel J, Schjoeth-Eskesen C, El-Ali HH, Madsen J, Kjaer A. (64)Cu-NODAGA-c (RGDyK) Is a Promising New Angiogenesis PET Tracer: correlation between Tumor Uptake and Integrin alpha(V)beta(3) Expression in Human Neuroendocrine Tumor Xenografts. *Int J Mol Imaging* (2012); **2012**: 379807.
- Panin VY, Kehren F, Michel C, Casey M. Fully 3-D PET reconstruction with system matrix derived from point source measurements. *IEEE Trans Med Imaging* (2006); **25**: 907–921.
- Pedersen SF, Graebe M, Fisker Hag AM, Hojgaard L, Sillesen H, Kjaer A. Gene expression and 18FDG uptake in atherosclerotic carotid plaques. *Nucl Med Commun* (2010); **31**: 423–429.
- Pedersen SF, Graebe M, Hag AM, Hoejgaard L, Sillesen H, Kjaer A. Microvessel Density But Not Neovascularization Is Associated with (18)F-FDG Uptake in Human Atherosclerotic Carotid Plaques. *Mol Imaging Biol* (2012); **14**: 384–392.
- Pedersen SF, Graebe M, Hag AM, Hoejgaard L, Sillesen H, Kjaer A. Microvessel density

- but not neoangiogenesis is associated with 18F-FDG uptake in human atherosclerotic carotid plaques. *Mol Imaging Biol* (2012); **14**: 384–392.
- Pedersen SF, Graebe M, Hag AM, Hoejgaard L, Sillesen H, Kjaer A. ¹⁸F-FDG imaging of human atherosclerotic carotid plaques reflects gene expression of the key hypoxia marker HIF-1 α . *Am J Nucl Med Mol Imaging* (2013); **3**: 384–392.
- Phelps ME, Hoffman EJ, Mullani NA, Ter-Pogossian MM. Application of annihilation coincidence detection to transaxial reconstruction tomography. *J Nucl Med* (1975); **16**: 210–224.
- Pohle K, Notni J, Bussemer J, Kessler H, Schwaiger M, Beer AJ. 68 Ga-NODAGA-RGD is a suitable substitute for (18)F-Galacto-RGD and can be produced with high specific activity in a cGMP/GRP compliant automated process. *Nucl Med Biol* (2012); **39**: 777–784.
- Polycarpou I, Thielemans K, Manjeshwar R, Aguiar P, Marsden PK, Tsoumpas C. Comparative evaluation of scatter correction in 3D PET using different scatter-level approximations. *Ann Nucl Med* (2011); **25**: 643–649.
- Rahaman SO, Lennon DJ, Febbraio M, Podrez EA, Hazen SL, Silverstein RL. A CD36-dependent signaling cascade is necessary for macrophage foam cell formation. *Cell Metab* (2006); **4**: 211–221.
- Reivich M, Kuhl D, Wolf A, Greenberg J, Phelps M, Ido T, Casella V, Fowler J, Gallagher B, Hoffman E, Alavi A, Sokoloff L. Measurement of local cerebral glucose metabolism in man with 18F-2-fluoro-2-deoxy-d-glucose. *Acta Neurol Scand Suppl* (1977); **64**: 190–191.
- Ribatti D, Levi-Schaffer F, Kovanen PT. Inflammatory angiogenesis in atherogenesis—a double-edged sword. *Ann Med* (2008); **40**: 606–621.
- Ripa RS, Knudsen A, Hag AM, Lebech AM, Loft A, Keller SH, Hansen AE, von Benzon E, Hojgaard L, Kjaer A. Feasibility of simultaneous PET/MR of the carotid artery: first clinical experience and comparison to PET/CT. *Am J Nucl Med Mol Imaging* (2013); **3**: 361–371.
- Rominger A, Saam T, Vogl E, Ubleis C, la Fougère C, Forster S, Haug A, Cumming P, Reiser MF, Nikolaou K, Bartenstein P, Hacker M. In vivo imaging of macrophage activity in the coronary arteries using 68 Ga-DOTATATE PET/CT: correlation with coronary calcium burden and risk factors. *J Nucl Med* (2010); **51**: 193–197.
- Ross R. Atherosclerosis—an inflammatory disease. *N Engl J Med* (1999); **340**: 115–126.
- Rudd JH, Warburton EA, Fryer TD, Jones HA, Clark JC, Antoun N, Johnstrom P, Davenport AP, Kirkpatrick PJ, Arch BN, Pickard JD, Weissberg PL. Imaging atherosclerotic plaque inflammation with [¹⁸F]-fluorodeoxyglucose positron emission tomography. *Circulation* (2002); **105**: 2708–2711.
- Rudd JH, Myers KS, Bansilal S, Machac J, Rafique A, Farkouh M, Fuster V, Fayad ZA. (18)Fluorodeoxyglucose positron emission tomography imaging of atherosclerotic plaque inflammation is highly reproducible: implications for atherosclerosis therapy trials. *J Am Coll Cardiol* (2007); **50**: 892–896.
- Rudd JH, Myers KS, Bansilal S, Machac J, Pinto CA, Tong C, Rafique A, Hargeaves R, Farkouh M, Fuster V, Fayad ZA. Atherosclerosis inflammation imaging with 18F-FDG PET: carotid, iliac, and femoral uptake reproducibility, quantification methods, and recommendations. *J Nucl Med* (2008); **49**: 871–878.
- Rudd JH, Myers KS, Bansilal S, Machac J, Woodward M, Fuster V, Farkouh ME, Fayad ZA. Relationships among regional arterial inflammation, calcification, risk factors, and biomarkers: a prospective fluorodeoxyglucose positron-emission tomography/computed tomography imaging study. *Circ Cardiovasc Imaging* (2009); **2**: 107–115.
- Schlemmer HP, Pichler BJ, Schmand M, Burbar Z, Michel C, Ladebeck R, Jattke K, Townsend D, Nahmias C, Jacob PK, Heiss WD, Claussen CD. Simultaneous MR/PET imaging of the human brain: feasibility study. *Radiology* (2008); **248**: 1028–1035.
- Shreve PD, Anzai Y, Wahl RL. Pitfalls in oncologic diagnosis with FDG PET imaging: physiologic and benign variants. *Radiographics* (1999); **19**: 61–77.
- Sluijter JC, Gasc JM, van Wanroij JL, Kisters N, Groeneweg M, Sollewijn Gelpke MD, Cleutjens JP, van den Akker LH, Corvol P, Wouters BG, Daemen MJ, Bijnens AP. Hypoxia, hypoxia-inducible transcription factor, and macrophages in human atherosclerotic plaques are correlated with intraplaque angiogenesis. *J Am Coll Cardiol* (2008); **51**: 1258–1265.
- Soret M, Bacharach SL, Buvat I. Partial-volume effect in PET tumor imaging. *J Nucl Med* (2007); **48**: 932–945.
- Tahara N, Kai H, Ishibashi M, Nakaura H, Kaide H, Baba K, Hayabuchi N, Imaizumi T. Simvastatin attenuates plaque inflammation: evaluation by fluorodeoxyglucose positron emission tomography. *J Am Coll Cardiol* (2006); **48**: 1825–1831.
- Takahashi N, Fujibayashi Y, Yonekura Y, Welch MJ, Waki A, Tsuchida T, Sadato N, Sugimoto K, Itoh H. Evaluation of ⁶²Cu labeled diacetyl-bis(N4-methylthiosemicarbazone) as a hypoxic tissue tracer in patients with lung cancer. *Ann Nucl Med* (2000); **14**: 323–328.
- Tatsumi M, Cohade C, Nakamoto Y, Wahl RL. Fluorodeoxyglucose uptake in the aortic wall at PET/CT: possible finding for active atherosclerosis. *Radiology* (2003); **229**: 831–837.
- Tawakol A, Migrino RQ, Bashian GG, Bedri S, Vermylen D, Cury RC, Yates D, LaMuraglia GM, Furie K, Houser S, Gewirtz H, Muller JE, Brady TJ, Fischman AJ. In vivo 18F-fluorodeoxyglucose positron emission tomography imaging provides a noninvasive measure of carotid plaque inflammation in patients. *J Am Coll Cardiol* (2006); **48**: 1818–1824.
- Ter-Pogossian MM, Phelps ME, Hoffman EJ, Mullani NA. A positron-emission transaxial tomograph for nuclear imaging (PETT). *Radiology* (1975); **114**: 89–98.
- Valk PE, Mathis CA, Prados MD, Gilbert JC, Budinger TF. Hypoxia in human gliomas: demonstration by PET with fluorine-18-fluoromisonidazole. *J Nucl Med* (1992); **33**: 2133–2137.
- Vallabhajosula S, Fuster V. Atherosclerosis: imaging techniques and the evolving role of nuclear medicine. *J Nucl Med* (1997); **38**: 1788–1796.
- Van de Wiele C, Lahorte C, Vermeersch H, Loose D, Mervillie K, Steinmetz ND, Vanderheyden JL, Cuvelier CA, Slegers G, Dierck RA. Quantitative tumor apoptosis imaging using technetium-99 m-HYNIC annexin V single photon emission computed tomography. *J Clin Oncol* (2003); **21**: 3483–3487.
- Virmani R, Kolodgie FD, Burke AP, Finn AV, Gold HK, Tulenko TN, Wrenn SP, Narula J. Atherosclerotic plaque progression and vulnerability to rupture: angiogenesis as a source of intraplaque hemorrhage. *Arterioscler Thromb Vasc Biol* (2005); **25**: 2054–2061.
- Vita JA. Endothelial function. *Circulation* (2011); **124**: e906–e912.
- Von Schulthess GK, Steinert HC, Hany TF. Integrated PET/CT: current applications and future directions. *Radiology* (2006); **238**: 405–422.
- Warburg O, Posener E, Negelein E. Über den stoffwechsel der Carcinomzelle. *Biochem Z* (1924); **152**: 309–344.
- Wasselius J, Larsson S, Jacobsson H. Time-to-time correlation of high-risk atherosclerotic lesions identified with [(18)F]-FDG-PET/CT. *Ann Nucl Med* (2009a); **23**: 59–64.
- Wasselius J, Larsson S, Sundin A, Jacobsson H. Assessment of inactive, active and mixed atherosclerotic plaques by 18F-FDG-PET; an age group-based correlation with cardiovascular risk factors. *Int J Cardiovasc Imaging* (2009b); **25**: 133–140.
- Watson KE, Bostrom K, Ravindranath R, Lam T, Norton B, Demer LL. TGF-beta 1 and

- 25-hydroxycholesterol stimulate osteoblast-like vascular cells to calcify. *J Clin Invest* (1994); **93**: 2106–2113.
- WHO. *World Health Statistics 2012*, pp. 33–85 (2012). World Health Organization. Ref Type: Online Source.
- Wu YW, Kao HL, Huang CL, Chen MF, Lin LY, Wang YC, Lin YH, Lin HJ, Tzen KY, Yen RF, Chi YC, Huang PJ, Yang WS. The effects of 3-month atorvastatin therapy on arterial inflammation, calcification, abdominal adipose tissue and circulating biomarkers. *Eur J Nucl Med Mol Imaging* (2012); **39**: 399–407.
- Yan J, Stringer SE, Hamilton A, Charlton-Meyns V, Gotting C, Muller B, Aeschlimann D, Alexander MY. Decorin GAG synthesis and TGF-beta signaling mediate Ox-LDL-induced mineralization of human vascular smooth muscle cells. *Arterioscler Thromb Vasc Biol* (2011); **31**: 608–615.
- Yun M, Yeh D, Araujo LI, Jang S, Newberg A, Alavi A. F-18 FDG uptake in the large arteries: a new observation. *Clin Nucl Med* (2001); **26**: 314–319.